



Ionic liquid assisted synthesis of nano Pd–Au particles and application for the detection of epinephrine, dopamine and uric acid

Tsung-Hsuan Tsai, Soundappan Thiagarajan, Shen-Ming Chen*, Ching-Yi Cheng

Electroanalysis and Bioelectrochemistry Laboratory, Department of Chemical Engineering and Biotechnology, National Taipei University of Technology, No.1, Section 3, Chung-Hsiao East Road, Taipei 106, Taiwan, ROC

ARTICLE INFO

Article history:

Received 25 February 2011

Received in revised form 30 October 2011

Accepted 3 November 2011

Available online 11 November 2011

Keywords:

Nanoparticles

Palladium

Gold

Ionic liquid

Epinephrine

Dopamine

Ascorbic acid

Uric acid

ABSTRACT

Nano Pd–Au particles have been electrochemically fabricated utilizing ionic liquid as green electrolyte (1-Butyl-3-methylimidazolium tetrafluoroborate). Nano Pd–Au particles modified glassy carbon electrode (GCE) and indium tin oxide coated glass electrodes were examined using atomic force microscopy, field emission scanning electron microscope and X-ray diffraction studies. Electrodeposited nano Pd–Au particles' average diameter was found as 33 nm. Nano Pd–Au particle modified GCE was electrochemically active and stable in various pH solutions. The proposed nano particle modified GCE reduces the over potential and shows the well defined oxidation peaks for the detection of epinephrine and simultaneous determination of dopamine and uric acid (in pH 7.0 phosphate buffer solution) using cyclic voltammetry and differential pulse voltammetry.

© 2011 Elsevier B.V. All rights reserved.

1. Introduction

Epinephrine (EP) is the most important neurotransmitter in the central nervous system and responsible for the various types of biological and chemical processes [1,2]. Thus the detection and determination of EP is an important criterion in the biological fluids and in pharmaceutical analysis. In biological fluids, EP always co-exists together with AA. Both compounds' oxidation potentials were very close and the electroanalysis process results in the overlapped voltammetric response at the bare electrodes.

To overcome this type of query, film modified electrodes have been found as suitable for the detection of EP [3–7]. Dopamine (DA) is a well known catecholamine neurotransmitter, and plays a significant role in the central nervous and hormones in the mammalian system. DA deficiency may result in neurological disorders such as Parkinson's disease and schizophrenia. Next the uric acid (UA) is an important end product in the human metabolism. The abnormal level of UA has resulted in kidney, leishmaniasis, gout and hyperuricemia disorders in the human beings. Thus the simultaneous detection of UA and DA is an important study in the clinical and pathological research [8–21].

Enzyme based biosensors are well known for the detection of EP, DA and UA. For example, tyrosinase-modified solid carbon paste electrode (SCPE) based amperometric sensor for the determination of catecholamines [22], enzyme micro sensors for the detection of dopamine and glutamate [23], urate oxidase–peroxidase coupled enzyme biosensor [24], uricase layer-by-layer films [25], uricase-immobilized eggshell membrane biosensor [26] and enzyme–ZnO nanoparticles-multiwall carbon nanotubes modified sensor for the uric acid determination [27] were reported.

Further the nanomaterial based electrode modifications are also utilized for the detection and determination of EP, DA and UA. Especially, nanoparticle based biosensors show interesting results for the detection and determination of EP, DA and UA. For example, self-assembled gold nanoparticles [5], gold electrodes modified with sulfur functionalized gold nanoparticles [28], Pd nanoparticle modified glassy carbon electrode (GCE) for the detection of epinephrine [29], gold nanoparticle–choline [21], nafion–Pt nano [30], PtAu hybrid film modified GCE [31], nanostructured metal particle-modified electrodes [32] and palladium nanoparticles-loaded carbon nanofibers modified electrode [33] for the detection of AA, DA and UA were reported. These details clearly show that the nanoparticle based biosensors were compatible for the detection and determination of EP, DA and UA.

Green chemistry also known as sustainable chemistry as a different research area shows the importance of research, pathway, and materials which reduce the use and generation of hazardous materials. In

* Corresponding author. Tel.: +886 2 27017147; fax: +886 2 27025238.
E-mail address: smchen78@ms15.hinet.net (S.-M. Chen).

electrochemistry, various types of solvents were used as electrolytes for the electrochemical applications. Majority of solvents were environmentally toxic and their utilization will create undesirable changes in the environment. Step by step development and utilization of nonhazardous solvents (green solvents) will be beneficial to maintain the clean environment. Therefore, utilization of green solvents in electrochemistry was found as an interesting and potential research. Recently, room temperature ionic liquids (RTILs) have been described as green electrolytes because; they have the characteristics of higher ionic conductivity with the wider electrochemical applications. Thus, here we have focused on the green synthesis and attempted to fabricate the nanomaterials using the ionic liquids as green electrolyte [34]. We employed 1-Butyl-3-methylimidazolium tetrafluoroborate (BMT) as green electrolyte for the electrochemical fabrication of nano Pd–Au particles at the different types of electrode surfaces. Further the nano Pd–Au particle modified GCE was directly employed for the detection of biologically important compounds (EP, DA and UA) in the physiological pH conditions (phosphate buffer solution (PBS) of pH 7.0). The proposed nano Pd–Au particle modified GCE exhibits the electrochemical signals for the detection of EP, DA, UA using cyclic voltammetry (CV), differential pulse voltammetry (DPV) and amperometric techniques.

2. Experimental details

1-Butyl-3-methylimidazolium tetrafluoroborate (BMT) (purity >97%, HPLC), palladium (II) chloride, anhydrous, 58–60%, epinephrine (EP), dopamine (DA), ascorbic acid (AA), glucose and p-acetamidophenol (AP) were purchased from Sigma-Aldrich (USA). Potassium tetrachloroaurate (III) hydrate (98%) was purchased from Strem Chemicals (USA). All other chemicals (Merck) used were of analytical grade (99%). Double distilled deionized water was used to prepare all the solutions. A phosphate buffer solution (PBS) of pH 7.0 was prepared using Na_2HPO_4 (0.05 mol l^{-1}) and NaH_2PO_4 (0.05 mol l^{-1}). Pure nitrogen was passed through all the experimental solutions. The adrenalin injection solution (epinephrine 1 mg ml^{-1}) was obtained from a local drug store. All the electrochemical experiments were performed using CHI 410a potentiostat (CH Instruments, USA). The BAS GCE ($\varphi=0.3 \text{ cm}$ in diameter, exposed geometric surface area 0.07 cm^2 , Bioanalytical Systems, Inc., USA) was used. A conventional three-electrode system was used which consists of Ag/AgCl (saturated KCl) as a reference, bare or nano Pd–Au particle modified GCE as working and platinum wire as counter electrode. Particularly, for nano Pd–Au particle deposition process ionic liquid employed (BMT) Ag electrode (Ag/ionic liquid) has been used as the reference. In the rest of the electrochemical studies, Ag/AgCl (saturated KCl) was used as a reference. Electrochemical impedance studies (EIS) were performed using ZAHNER impedance analyzer (Germany). The atomic force microscopy (AFM) images were recorded with multimode scanning probe microscope (CSPM-4000, Being Nano-Instruments, Beijing, China). AFM tapping mode has been employed for the surface analysis. A silicon cantilever (Ultrasharp, NSC15/AIBS, MikroMasch) was used with a resonant frequency of 325 kHz and a spring constant of 40 N/m. Field emission scanning electron microscope (FE-SEM) images were performed using HITACHI S-4700 (Japan) (5 kV). X-ray diffraction (XRD) experiment was done using XPERT-PRO (PANalytical B.V., The Netherlands) using $\text{Cu K}\alpha$ radiation ($k=1.54 \text{ \AA}$). The DPV parameters employed for the simultaneous determination of DA and UA were as follows; Init E (V) = -0.8 , Final E (V) = 1.2 , Incr E (V) = 0.004 , Amplitude (V) = 0.05 , Pulse width (s) = 0.05 , and pulse period (s) = 0.2 .

Prior to the electrochemical deposition process, the GCE was well polished with the help of BAS polishing kit with aqueous slurries of alumina powder ($0.05 \mu\text{m}$), rinsed and ultrasonicated in double distilled deionized water. The precursor solution for the film deposition process has been prepared using ionic liquid (BMT) (1 ml BMT contains 1 mM KAuCl_4 and 1 mM PdCl_2). The Pd–Au particles have been electrochemically deposited by immersing the pretreated GCE in

1 ml BMT containing 1 mM KAuCl_4 and 1 mM PdCl_2 and the potential cycling has been applied between 1.0 and -1.0 V at the scan rate of 0.05 V/s for five cycles [29]. Further the Pd–Au particle modified GCE was washed with deionized water, dried for 5 min and employed for the further investigations.

3. Results and discussion

3.1. AFM and SEM analyses

Electrodeposited Pd–Au particles have been examined using AFM and FE-SEM techniques (Fig. 1(A) and (B)). AFM tapping mode has been employed for the surface analysis of Pd–Au particle deposited GCE surface. Fig. 1(A) shows the 2D magnified view of Pd–Au particle modified GCE. Fig. 1(B) shows the FE-SEM image of the Pd–Au particle modified indium tin oxide coated glass electrode (ITO). From Fig. 1(A) and (B), we can see the electrodeposited Pd–Au particles in obvious manner in the average size range of 10 to 50 nm. Hereafter the Pd–Au particles are denoted as nano Pd–Au particles. Fig. 1(C) shows the granularity normal distribution chart of the nano Pd–Au particles electrodeposited on GCE. The average height of nano Pd–Au particles was found as 11.5 nm and the maximum number of nano Pd–Au particles exhibits

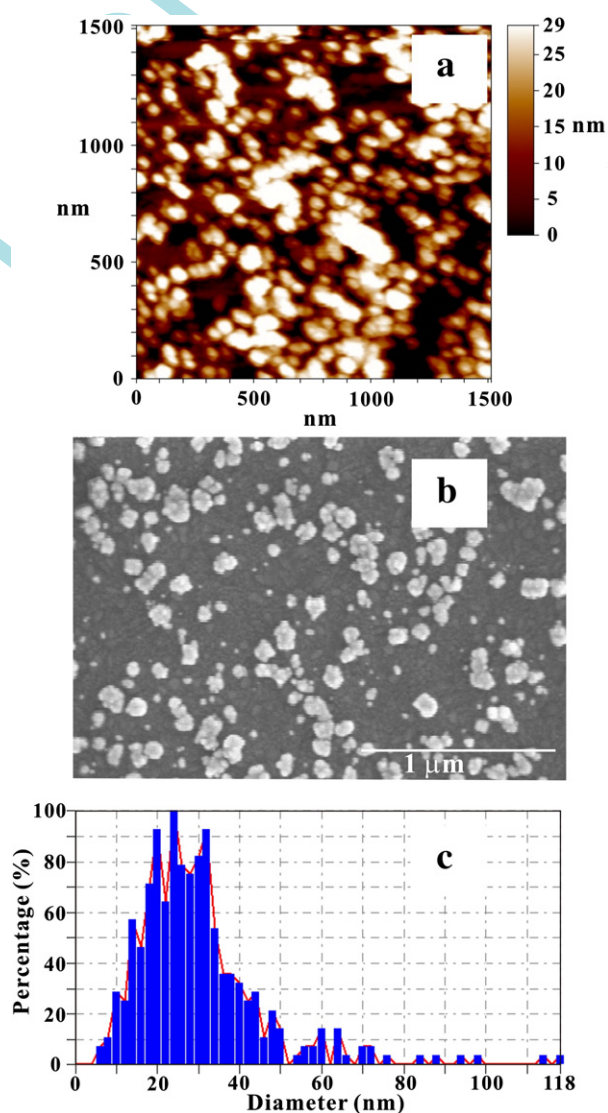


Fig. 1. (a) AFM two dimensional view of nano Pd–Au particle modified GCE, (b) FE-SEM image of nano Pd–Au particle modified ITO. (c) Granularity normal distribution chart of the nano Pd–Au particle modified GCE.

in 20 nm heights, respectively. Based on the granularity normal distribution chart (Fig. 1C), the average diameter of nano Pd–Au particles has been found as 33 nm. The total number of nano Pd–Au particles found within the 1500×1500 nm surface area was 330.

3.2. XRD analysis

Fig. 2(A) represents the XRD pattern of nano Pd–Au particle modified ITO. In Fig. 2(A), two peaks appear at around 38° (2θ) corresponds to the (111) crystallographic plane and the peak at around 45° (2θ) corresponds to the (200) plane. Here the crystallographic surface (111) has been assigned for the Au ($2\theta = 37.32^\circ$) and the crystallographic surface (200) plane has been assigned for the two peaks ($2\theta = 44.77^\circ$ and 46.18°). This XRD pattern confirms the presence of Au and Pd particles on the ITO surface [35,36]. Here the electrodeposited Pd–Au may be present in the form of alloy or single metal particles. Therefore, here we generally claim the electrodeposited particles as nano Pd–Au particles. Also, Table 1 shows the numerous possibilities of Pd and Au based nanomaterial synthesis using various methods. Based on this comparison (Table 1), the proposed electrochemical method is found as a direct method and the fabricated nanoparticles fall in the higher size dimension, respectively. Comparing with other methods this method is found as a direct one because of the easy fabrication process. Further chemical synthesis needs more sophisticated experimental conditions for the fabrication of nanomaterials. At the same time, electrochemical deposition method was found as the easiest and convenient for this type of nanomaterial fabrication process. Also, nano Pd–Au particle modified electrodes

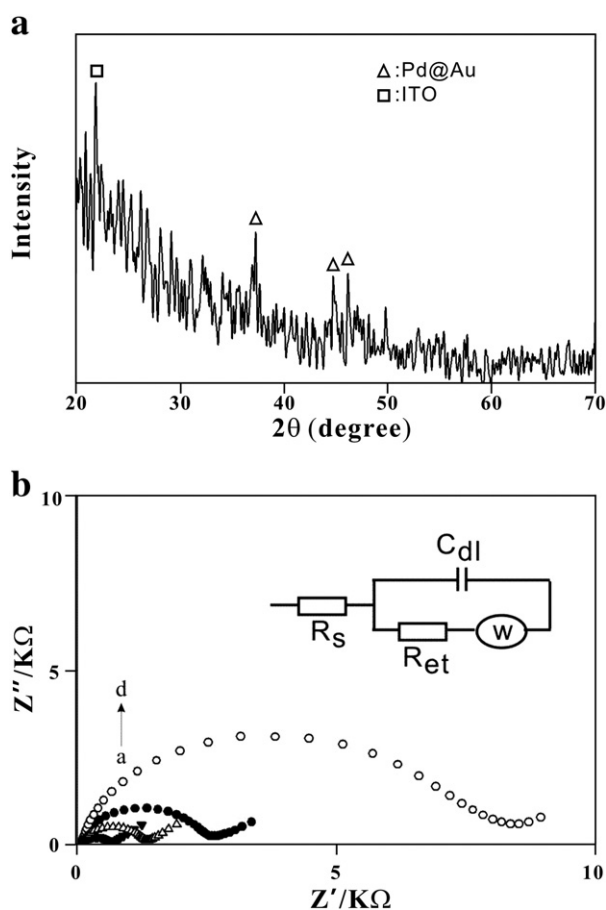


Fig. 2. (A) XRD patterns of nano Pd–Au particle modified ITO. (B) Electrochemical impedance spectra curves of (a) bare GCE (b) nano Pd–Au particles and (c) nano Au (1st layer) Pd (2nd layer) (d) nano Pd (1st layer) nano Au (2nd layer) modified GCE (in 0.1 M pH 7.0 PBS containing 5×10^{-3} M $[\text{Fe}(\text{CN})_6]^{3-/4-}$).

Table 1

Comparison table for nano particle synthesis method.

| Type of nanomaterial | Method | Particle size (nm) | Ref |
|---|----------------------------|--------------------|-----------|
| Au/Pd bimetallic nanoparticles | Thermal relaxation | 3.2–5.3 | [37] |
| Au–Pd nanoparticles | Sono chemical | 8 | [38] |
| Au–Pd (core–shell) nanoparticles | Ultrasonic irradiation | 9 | [39] |
| Au@Pd nanoparticles | Chemical synthesis | 0.7–50 | [40] |
| Au@Pd nanoparticles | Alumina matrix sol | 4.5–13 | [41] |
| Au@Pd core–shell nano octahedron shaped particles | Aqueous synthesis | $41.1 \pm (3.5)$ | [42] |
| Pd@Au nanoparticles | Chemical synthesis | 4–7 | [43] |
| Pd–Au nanoparticles | Electrochemical deposition | 10–50 | This work |

could be directly employed for the electrochemical analysis. Therefore, here we have employed electrochemical deposition method for the fabrication of nano Pd–Au particles.

3.3. EIS analysis

Electrochemical activity of the nano Pd–Au particle modified GCE has been examined using EIS technique. Impedance spectroscopy is an effective method to probe the features of surface modified electrodes. Here Fig. 2(B) shows the faradaic impedance spectra, presented as Nyquist plots (Z'' vs. Z') for the bare (curve a), nano Pd–Au particles (curve b), nano Au (1st layer) Pd (2nd layer) (curve c) and nano Pd (1st layer) nano Au (2nd layer) modified GCE (curve d). Here the bare GCE (curve a) exhibits a very small depressed semi circle arc ($R_{et} = 0.64$ ($Z'/K\Omega$)) that represents the characteristics of diffusion limited electron-transfer process on the electrode surface. At the same time, the nano Pd–Au particle modified GCE shows like a depressed semi circle arc with an interfacial resistance due to the electrostatic repulsion between the charged surface and probe molecule $[\text{Fe}(\text{CN})_6]^{3-/4-}$ (curve b). This depressed semi circle arc ($R_{et} = 1.34$ ($Z'/K\Omega$)) clearly indicates the electron transfer resistance behavior comparing with the bare GCE. At the same time, other different types of combinations were also examined using the EIS analysis. Here the Au (1st layer) Pd (2nd layer) modified GCE's R_{et} has been found as 2.64 ($Z'/K\Omega$) (curve c) and the Au (1st layer) Pd (2nd layer) modified GCE's R_{et} has been found as 8.51 ($Z'/K\Omega$) (curve d). Above discussed EIS results clearly show that the nano Pd–Au particle modified GCE (curve b) possesses the lower electron transfer resistance comparing with the other possible combinations, respectively.

3.4. Electrochemical characterization of nano Pd–Au particle modified GCE

The electrochemical response of nano Pd–Au particles was examined in pH 7.0 PBS. CV has been employed for the different scan rate studies. Fig. 3(A) represents the CV response of nano Pd–Au particle modified GCE in pH 7.0 PBS. Nano Pd–Au particles exhibit Au anodic peak at 0.93 V, Au cathodic peak and Pd cathodic peak responses at 0.48 and -0.31 V. Further the corresponding anodic and cathodic peak currents increase linearly with respect to the scan rate in the range of 0.01 to 0.1 V/s (a–j). Here the cathodic peak current for the Pd becomes much broader in the higher scan rates. The inset of Fig. 3(A) shows the plot of Au anodic and cathodic peak currents vs. scan rate. The corresponding linear regression equations for the Au anodic and cathodic peak currents vs. scan rate were expressed as I_{pc} (μA) = $13.73v$ (V/s) – 43.5, $R^2 = 0.997$ and I_{pa} (μA) = $4.127v$ (V/s) + 34.66, $R^2 = 0.973$. Here the linear increase in the anodic and cathodic peak currents with respect to the scan rate shows that the nano Pd–Au particles possess surface controlled thin-layer electrochemical behavior. Next the nano Pd–Au particle modified GCE has been examined in various pH solutions. Fig. 3(B) shows the CV response of nano Pd–Au particle

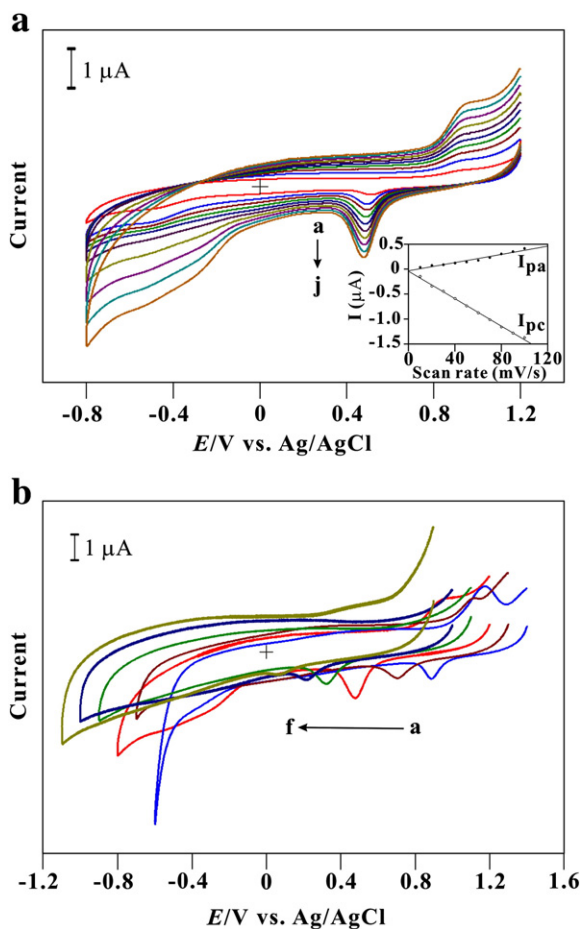


Fig. 3. (a) Different scan rate studies of nano Pd–Au particle modified GCE in 0.1 M pH 7.0 PBS. Scan rate in the range of a–j: 0.01–1 V/s. Inset shows the I_{pa} vs. scan rate. (b) Cyclic voltammetric response of nano Pd–Au particle modified GCE in different pHs (1, 4, 7, 9, 11 and 13).

modified GCE obtained in different pH conditions. This result clearly explicates that the nano Pd–Au particle modified GCE is electrochemically active and stable in various pH conditions (1, 4, 7, 9, 11 and 13).

3.5. Electrocatalytic detection of EP

The detection and determination of EP (Fig. 4) was performed using CV and amperometric methods. Fig. 4 shows CV response of nano Pd–Au particle modified GCE for the detection of EP in pH 7.0 PBS. As it can be seen in Fig. 4, the nano Pd–Au particle modified GCE exhibits a single oxidation peak at around 0.3 V for the electrocatalytic detection of EP. Here the catalytic peak potential for the EP electrooxidation is found at around 0.3 V for nano Pd–Au particle modified GCE, whereas the bare GCE exhibits a small diminished peak at 0.42 V. Thus, the nano Pd–Au particles reduce the over potential and are found to be effective for the electrocatalytic oxidation of EP. Also, there is an increase in the anodic peak current for the increasing concentrations of EP at nano Pd–Au particle modified GCE (Fig. 4, curve a–f). The inset of Fig. 4 shows the calibration plot for the EP detection at the nano Pd–Au particle modified GCE and the corresponding linear regression equation was found as $I_{pa} (\mu\text{A}) = 0.043 \text{ C (mg/L)} + 0.009$, with a correlation coefficient of $R^2 = 0.996$.

After the electrocatalysis, the nano Pd–Au particle modified GCE was stored in room temperature for 2 h and examined in pH 7.0 PBS. In this case, it showed 10% current decrease from its initial current value. At the same time, freshly prepared nano Pd–Au particle modified GCE's stability was examined. It was stored in room temperature for three days. After three days the nano Pd–Au particle modified GCE exhibits

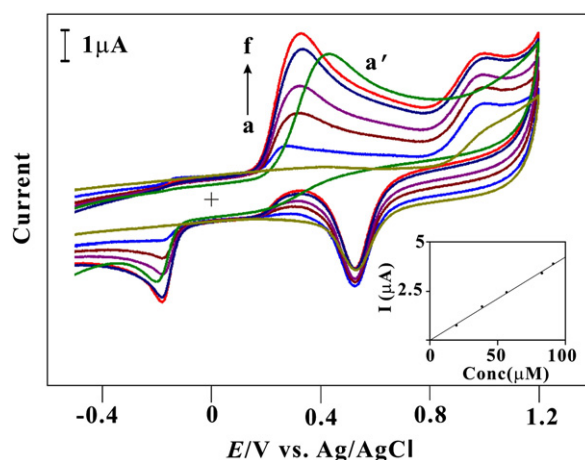


Fig. 4. CVs of nano Pd–Au particle modified GCE for the detection of epinephrine in pH 7.0 PBS. Epinephrine concentrations were in the range of: (a–f) 0, 19.6, 38.5, 56.6, 82.6 and 90.9 μM , (a') bare GCE = 90.9 μM (scan rate: 0.1 V/s). Inset shows the calibration plot for the determination of EP.

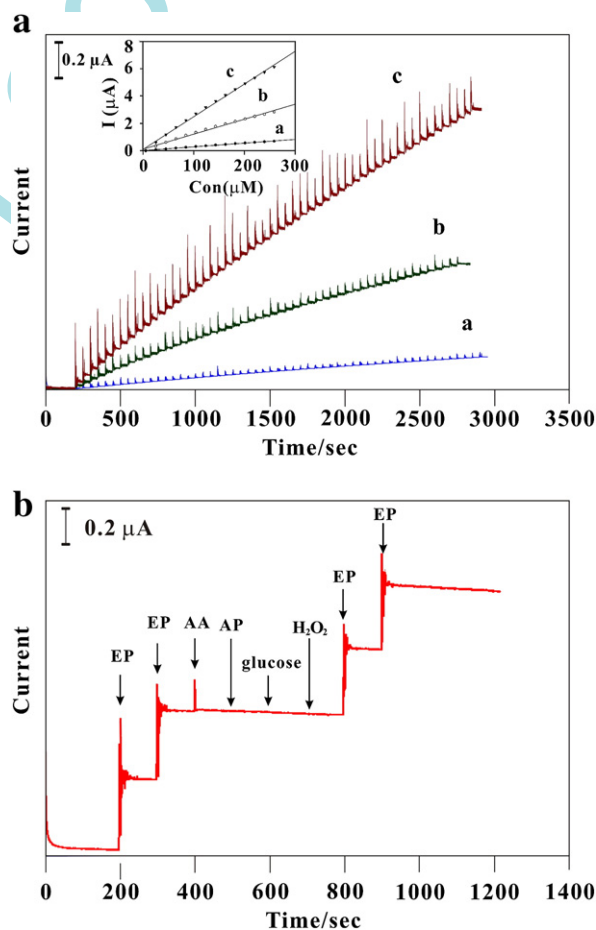


Fig. 5. (A) Amperometric determination of epinephrine on nano Pd–Au particle modified GCE in 0.1 M PBS (pH 7.0) at 0.3 V, rotation rate is 1000 rpm. Successive additions of epinephrine in the range of 5×10^{-6} to 2.60×10^{-4} M and inset figure shows the corresponding calibration plot of (a) bare GCE (b) nano Pd–Au particle modified GCE in lab sample and (c) nano Pd–Au particle modified GCE in real sample (injection solution). (B) Amperometric determination at nano Pd–Au particle modified GCE (in 0.1 M PBS (pH 7.0) at 0.3 V) for the successive additions of (a) EP (1×10^{-5} M), (b) EP (1×10^{-5} M), (c) AA (1×10^{-6} M), (d) AP (1×10^{-6} M), (e) glucose (1×10^{-6} M), (f) H_2O_2 (1×10^{-6} M), (g) EP (1×10^{-5} M) and (h) EP (1×10^{-5} M).

Table 2
Comparison table for the detection of EP detection.

| Type | Method | Buffer (PBS) (pH) | Potential (V) | EP | | Ref |
|----------------------------|-------------|----------------------|------------------|--|--|-----------|
| | | | | Linear range | | |
| Nano-gold/GCE ^a | CV | 7.0 | 0.2 | 1.0 × 10 ⁻⁶ –1.0 × 10 ⁻⁴ M | | [44] |
| Nano-Au electrode | CV | 7.0 | 0.18 | 1.0 × 10 ⁻⁷ –1.0 × 10 ⁻⁴ M | | [5] |
| Nanocomposite film/GCE | CV | 6.75 | 0.28 | 3.0 × 10 ⁻⁴ –1.0 × 10 ⁻³ M | | [45] |
| Au/PPyox/GCE ^b | DPV | 7.0 | 0.2 | 3.0 × 10 ⁻⁷ –2.1 × 10 ⁻⁵ M | | [46] |
| nano-Au/GCE | DPV | 7.0 | 0.13 | 1.0 × 10 ⁻⁷ –5.0 × 10 ⁻⁴ M | | [47] |
| Nano Pd/GCE | DPV | 7.0 | 0.2 | 34–349 μM | | [29] |
| Nano Pd–Au particles/GCE | Amperometry | 7.0 | 0.3 | 50–260 μM | | This work |

^a GCE—glassy carbon electrode.

^b PPyox—polypyrrole.

as stable with 5% current decrease from its initial value. These evaluations clearly validate the stability and reusable nature of the nano Pd–Au particle modified GCE.

Amperometric response of nano Pd–Au particles modified GCE for EP determination was investigated in pH 7.0 PBS (at 0.3 V). Fig. 5(A) shows typical current vs. time curve for successive additions of EP (5.0 × 10⁻⁶–2.6 × 10⁻⁴ M) at the bare (a), nano Pd–Au particles (EP stock solution (lab sample)) (b), and nano Pd–Au particle modified GCE (EP injection solution (real sample)) (c). Here the Pd–Au particle modified GCE showed immediate response for the sequential additions of EP and reached another steady-state current within 5 s for the lab and real samples. This result clearly explicates the capability of the Pd–Au

particles for the determination of EP. Further the inset of Fig. 5(A) shows the calibration curves for the EP determination at bare (a), nano Pd–Au particles (in lab sample) (b), and nano Pd–Au particle modified GCE (in real sample) (c). Finally, the nano Pd–Au particle modified GCE shows good linear response for the electrocatalytic oxidation of EP in the range of 5 × 10⁻⁶–2.6 × 10⁻⁴ M with the lowest detection limit of 5 × 10⁻⁶ M, respectively. Table 2 shows the comparison chart for the EP detection based on nanomaterial modified electrodes.

Selectivity of the nano Pd–Au particle modified GCE was examined using amperometric method (Fig. 5(B)). Amperometric response was obtained for the successive injections of EP (1 × 10⁻⁵ M), ascorbic acid (AA) (1 × 10⁻⁶ M), acetaminophen (AP) (1 × 10⁻⁶ M), glucose (1 × 10⁻⁶ M) and H₂O₂ (1 × 10⁻⁶ M) in pH 7.0 PBS (0.3 V). Here, except AA, all the remaining compounds don't exhibit any interference signals and for the further additions of EPs the current response is clearly increasing at nano Pd–Au particle modified GCE. This shows the specific nature and capability of the nano Pd–Au particle modified GCE which overcomes the interference signals and shows only the detection signals for EP.

3.6. Simultaneous determination of DA and UA

Simultaneous determination of DA and UA at nano Pd–Au particle modified GCE was investigated using DPV (Fig. 6). Nano Pd–Au particle modified GCE exhibits well-defined two separate anodic peaks for the determination of DA and UA (Fig. 6). Here the nano Pd–Au particles resolve the mixed voltammetric response of these species (DA and UA) into two well-defined voltammetric peaks at 0.15 and 0.53 V. Further the peak separations between DA and UA (0.38 V) are sufficient enough to exhibit them as well-defined two separate peaks. Here all the oxidation peak currents of DA and UA were increasing linearly with respect to their concentrations, respectively. Simultaneous determination of these compounds' (DA and UA) concentrations were in the linear range of 0.5–6.95 × 10⁻⁶ and

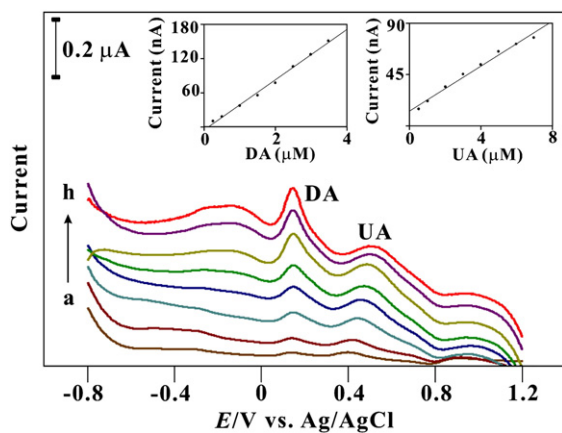


Fig. 6. Simultaneous determination of DA and UA on nano Pd–Au particle modified GCE. DA and UA concentrations were in the linear range of DA (a–h: 0.5, 1, 2, 2.99, 3.98, 4.97, 5.96, 6.95 × 10⁻⁶ M) and UA (a–h: 0.25, 0.49, 0.99, 1.49, 1.99, 2.48, 2.98 and 3.47 × 10⁻⁶ M) (a' bare GCE; DA and UA; 6.95 × 10⁻⁶ and 3.47 × 10⁻⁶ M). Inset shows the calibration plot for the determination of DA and UA.

Table 3
Comparison table for the detection of DA and UA.

| Type | Method | pH (PBS) | Potential (V) | | Linear range | | Ref |
|---|--------|-------------|---------------|------|--|--|-----------|
| | | | DA | UA | DA | UA | |
| GC/Nf/Pt nano electrode ^a | DPV | | 0.13 | – | 3–60 μM | – | [30] |
| PtAu hybrid film/GCE | CV | 7.0 | 0.37 | 0.54 | 0.022–0.440 mM | 0.062–2.49 mM | [31] |
| | DPV | | | | 0.024–0.384 mM | 0.021–0.33 mM | |
| GNP/Ch/GCE ^{b, c} | DPV | 7.0 | 0.23 | 0.37 | 0.2–80 μM | 1.2–100 μM | [21] |
| AuNPs/P3MT/GCE ^d | DPV | 7.0 | 0.19 | 0.34 | 1–35 μM | 1–32 μM | [48] |
| Pt/PMT(BE)/Pd(CV) electrode ^{e, f} | DPV | 7.4 | 0.11 | – | 0.05–1 μM | – | [49] |
| Cu/PPy/GCE | DPV | 7.0 | 0.17 | 0.36 | 1 × 10 ⁻⁹ –1 × 10 ⁻⁷ M | 1 × 10 ⁻⁹ –1 × 10 ⁻⁵ M | [50] |
| Nano Pd–Au particles/GCE | DPV | 7.0 | 0.15 | 0.53 | 0.5–6.95 μM | 0.25–3.47 μM | This work |

^a Nf—nafion.

^b GNP—gold nanoparticle.

^c Ch—choline.

^d P3MT—poly(3-methylthiophene).

^e PMT—poly(3-methylthiophene).

^f BE—bulk electrolysis.

$0.25\text{--}3.47 \times 10^{-6}$ M. From the calibration plots, the linear regression equations for the simultaneous determination of DA and UA at nano Pd–Au particle modified GCE were expressed as $I_{pa} \text{ (nA)} = 44.06 \text{ C (} 10^{-6} \text{ M)} - 4.905$, $R^2 = 0.995$ and $I_{pa} \text{ (nA)} = 9.854 \text{ C (} 10^{-6} \text{ M)} - 13.13$, $R^2 = 0.986$. Relative standard deviations for these compounds' determination were less than 5.1% which shows the efficiency and linear nature of nano Pd–Au particle modified GCE. Also, Table 3 clearly shows that nano Pd–Au particle modified GCE possesses the sufficient linear range for the simultaneous detection of DA and UA comparing with previous literature reports, respectively.

4. Conclusion

Here we report a simple method for the electrochemical fabrication of stable nano Pd–Au particles (using ionic liquid (BMT) as green electrolyte) modified GCE and ITO. The electrodeposited nano Pd–Au particles have been characterized using AFM, FE-SEM, EIS and XRD studies. The nano Pd–Au particle modified GCE has been found as effective for the detection and determination of EP, DA and UA in physiological pH conditions. Overall, the proposed nano Pd–Au particles are very easy to fabricate using ionic liquids as green electrolyte, eco-friendly, and could be applied for the various types of EP, DA and UA electrocatalytic oxidation related studies.

Acknowledgment

This work was supported by National Science Council of Taiwan (ROC).

References

- [1] Q.M. Xue, *Physiological and Pathological Chemistry of Nervous System*, Science Press, Beijing, 1978, p. 102.
- [2] A. Sivanesan, S.A. John, *Electroanal.* 20 (2008) 2340.
- [3] A. Salimi, C.E. Banks, R.G. Compton, *Analyst* 129 (2004) 225.
- [4] H. Wang, D. Huang, R. Liu, *J. Electroanal. Chem.* 570 (2004) 83.
- [5] L. Wang, J. Bai, P. Huang, H. Wang, L. Zhang, Y. Zhao, *Electrochem. Commun.* 8 (2006) 1035.
- [6] J. Ni, H. Ju, H. Chen, D. Leech, *Anal. Chim. Acta* 378 (1999) 151.
- [7] H. Zhang, X. Zhou, R. Hui, N. Li, D. Liu, *Talanta* 56 (2002) 1081.
- [8] M. Ferreira, L.R. Dinelli, K. Wohnrath, A.A. Batista, O.N. Oliveira Jr., *Thin Solid Films* 446 (2004) 301.
- [9] T. Ahuja, Rajesh, D. Kumar, V.K. Tanwar, V. Sharma, N. Singh, A.M. Biradar, *Thin Solid Films* 519 (2010) 1128.
- [10] S.N.D. Jodi, F.C. Macro, L. Callum, D. James, *Electroanal.* 17 (2005) 1233.
- [11] S. Thiagarajan, T.H. Tsai, S.M. Chen, *Biosens. Bioelectron.* 24 (2009) 2712.
- [12] J. Zen, P. Chen, *Anal. Chem.* 69 (1997) 5087.
- [13] Y.L. Zeng, C.X. Li, C.R. Tang, X.B. Zhang, G.L. Shen, R.Q. Yu, *Electroanal.* 18 (2006) 440.
- [14] X.Q. Lin, G.F. Kang, L.P. Lu, *Bioelectrochemistry* 70 (2007) 235.
- [15] T. Selvaraju, R. Ramaraj, *J. Appl. Electrochem.* 33 (2003) 759.
- [16] X.H. Lin, Y.F. Zhang, W. Chen, P. Wu, *Sensor. Actuat. B Chem.* 122 (2007) 309.
- [17] H. Yao, Y.Y. Sun, X.H. Lin, Y.H. Tang, L.Y. Huang, *Electrochim. Acta* 52 (2007) 6165.
- [18] A.H. Liu, I. Honma, H.S. Zhou, *Biosens. Bioelectron.* 23 (2007) 74.
- [19] Y.F. Zhao, Y.Q. Gao, D.P. Zhan, H. Liu, Q. Zhao, Y. Kou, Y.H. Shao, M.X. Li, Q.K. Zhuang, Z.W. Zhu, *Talanta* 66 (2005) 51.
- [20] S.F. Jiao, M.G. Li, C. Wang, D.L. Chen, B. Fang, *Electrochim. Acta* 52 (2007) 5939.
- [21] P. Wang, Y.X. Li, X. Huang, L. Wang, *Talanta* 73 (2007) 431.
- [22] M. Pravda, C. Petit, Y. Michotte, J.-M. Kauffmann, K. Vyffas, *J. Chromatogr. A* 727 (1996) 47.
- [23] S. Cosnier, C. Innocent, L. Allien, S. Poitry, M. Tzacopoulos, *Anal. Chem.* 69 (1997) 968.
- [24] E. Akyilmaz, M.K. Sezgenturk, E. Dinckaya, *Talanta* 61 (2003) 73.
- [25] M.L. Moraes, U.P.R. Filho, O.N. Oliveira, M. Ferreira, *J. Solid State Electrochem.* 11 (2007) 1489.
- [26] Y. Zhang, G. Wen, Y. Zhou, S. Shuang, C. Dong, M.M.F. Choi, *Biosens. Bioelectron.* 22 (2007) 1791.
- [27] Y. Wang, L. Yu, Z. Zhu, J. Zhang, J. Zhu, *Anal. Lett.* 42 (2009) 775.
- [28] T. Luczak, *Electrochim. Acta* 54 (2009) 5863.
- [29] S. Thiagarajan, R.F. Yang, S.M. Chen, *Bioelectrochemistry* 75 (2009) 163.
- [30] T. Selvaraju, R. Ramaraj, *J. Electroanal. Chem.* 585 (2005) 290.
- [31] S. Thiagarajan, S.M. Chen, *Talanta* 74 (2007) 212.
- [32] R. Ramaraj, *J. Chem. Sci.* 118 (2006) 593.
- [33] J. Huang, Y. Liu, H. Hou, T. You, *Biosens. Bioelectron.* 24 (2008) 632.
- [34] T.H. Tsai, S. Thiagarajan, S.M. Chen, *J. Appl. Electrochem.* 40 (2010) 493.
- [35] T.J. Schmidt, Z. Jusys, H.A. Gasteiger, R.J. Behm, U. Endruschat, H. Boennemann, *J. Electroanal. Chem.* 501 (2001) 132.
- [36] C. Xu, Z. Tian, Z. Chen, S.P. Jiang, *Electrochem. Commun.* 10 (2008) 246.
- [37] S. Deki, K. Akamatsu, Y. Hatakenaka, M. Mizuhata, A. Kajinami, *Nanostruct. Mater.* 11 (1999) 59.
- [38] R. Oshima, T.A. Yamamoto, Y. Mizukoshi, Y. Nagata, Y. Maeda, *Nanostruct. Mater.* 12 (1999) 111.
- [39] N. Taguchi, F. Hori, T. Iwai, A. Iwase, T. Akita, S. Tanaka, *Appl. Surf. Sci.* 255 (2008) 164.
- [40] L. Cui, A. Wang, D.Y. Wu, B. Ren, Z.Q. Tian, *J. Phys. Chem. C* 112 (2008) 17618.
- [41] D. Jana, A. Dandapat, D. Goutam, *J. Phys. Chem. C* 113 (2009) 9101.
- [42] Y.W. Lee, M. Kim, Z.H. Kim, S.W. Han, *J. Am. Chem. Soc.* 131 (2009) 17036.
- [43] Y. Yang, X. Gong, H. Zeng, L. Zhang, X. Zhang, C. Zou, S. Huang, *J. Phys. Chem. C* 114 (2010) 256.
- [44] B. Jin, H. Zhang, *Anal. Lett.* 35 (2002) 1907.
- [45] U. Yogeswaran, S. Thiagarajan, S.M. Chen, *Anal. Biochem.* 365 (2007) 122.
- [46] J. Li, X.Q. Lin, *Anal. Chim. Acta* 596 (2007) 222.
- [47] Z. Yang, G. Hu, X. Chen, J. Zhao, G. Zhao, *Colloid. Surface. B* 54 (2007) 230.
- [48] X. Huang, Y. Li, P. Wang, L. Wang, *Anal. Sci.* 24 (2008) 1563.
- [49] N.F. Atta, M.F. El-Kady, *Sensor. Actuat. B* 145 (2010) 299.
- [50] S.U. Ulubay, Z. Dursun, *Talanta* 80 (2010) 1461.